Organic & Biomolecular Chemistry

Dynamic Article Links

Cite this: *Org. Biomol. Chem.*, 2011, **9**, 8400

www.rsc.org/obc

PAPER

Predicting Michael-acceptor reactivity and toxicity through quantum chemical transition-state calculations†

Denis Mulliner,[a,b] Dominik Wondrousch[a,b] and Gerrit Schüürmann*[a,b]

Received 1st July 2011, Accepted 2nd September 2011
DOI: 10.1039/c1ob06065a

The electrophilic reactivity of Michael acceptors is an important determinant of their toxicity. For a set of 35 α,β-unsaturated aldehydes, ketones and esters with experimental rate constants of their reaction with glutathione (GSH), k_{GSH}, quantum chemical transition-state calculations of the corresponding Michael addition of the model nucleophile methane thiol (CH_3SH) have been performed at the B3LYP/6-31G** level, focusing on the 1,2-olefin addition pathway without and with initial protonation. Inclusion of Boltzmann-weighting of conformational flexibility yields intrinsic reaction barriers $\Delta E^{\ddagger}$ that for the case of initial protonation correctly reflect the structural variation of k_{GSH} across all three compound classes, except that they fail to account for a systematic (essentially incremental) decrease in reactivity upon α-substitution. By contrast, the reduction in k_{GSH} through β-substitution is well captured by $\Delta E^{\ddagger}$. Empirical correction for the α-substitution effect yields a high squared correlation coefficient ($r^2 = 0.96$) for the quantum chemical prediction of log k_{GSH}, thus enabling an in silico screening of the toxicity-relevant electrophilicity of α,β-unsaturated carbonyls. The latter is demonstrated through application of the calculation scheme for a larger set of 46 Michael-acceptor aldehydes, ketones and esters with experimental values for their toxicity toward the ciliates *Tetrahymena pyriformis* in terms of 50% growth inhibition values after 48 h exposure (EC_{50}). The developed approach may add in the predictive hazard evaluation of α,β-unsaturated carbonyls such as for the European REACH (Registration, Evaluation, Authorization and Restriction of Chemicals) Directive, enabling in particular an early identification of toxicity-relevant Michael-acceptor reactivity.

Introduction

The Michael addition proceeds through reaction of a nucleophile, the Michael donor, with an electron-poor olefin, the Michael acceptor that is activated through electron-withdrawing substituents. Originally confined to enolate nucleophiles typically generated through base catalysis, non-enolate nucleophiles such as thiols and amines may also serve as Michael donors, in which case the reaction is often (but not necessarily) termed Michael-type addition. Recent interest concerns stereoselective and polymer-supported reaction pathways,[1–4] and reviews inform about the impact of α-carbon substitution as well as about a wide range of synthetic applications of Michael and Michael-type additions toward biomedical, pharmaceutical, optoelectronic and other macromolecular technologies.[5,6]

As electrophilic agents, Michael acceptors may form covalent bonds to nucleophilic sites of proteins and the DNA of biological organisms, resulting in diseases such as carcinogenicity,[7–9] allergic contact dermatitis,[10–12] and in excess toxicity (as compared to the unspecific narcosis or baseline toxicity) toward aquatic organisms.[13–17] Moreover, the Michael addition to endogenous cysteine thiol sites is involved in pathologies associated with atherosclerosis and oxidative stress,[18–22] in the anti-inflammatory activity of cyclopentenone prostaglandins,[23] in the activation of nerve system ion channels,[24] and in the induction of enzymes protecting against carcinogenesis.[25] As pointed out recently, there is indeed a substantial degree of overlap between protein and DNA reactivity in terms of respective electrophilic structural alerts,[26] providing further evidence for the fundamental electrophile–nucleophile reaction as molecular initiating event across different adverse outcome pathways.

Despite the toxicological potential of Michael acceptors due to their electrophilic reactivity, they may also induce phase-2 enzymes that protect against carcinogenesis.[24] Interestingly, this beneficial action is initiated through a Michael addition with endogenous thiol groups, with *ortho*-hydroxylated benzylidene-alkanones forming one respective example.[25]

Concerning α,β-unsaturated carbonyls, their Michael addition to a nucleophile NuH is often understood to proceed *via* a

[a]*UFZ Department of Ecological Chemistry, Helmholtz Centre for Environmental Research, Permoserstr. 15, 04318, Leipzig, Germany. E-mail: gerrit.schuurmann@ufz.de; Fax: +49-341-235-1785; Tel: +49-341-235-1262*
[b]*Institute for Organic Chemistry, Technical University Bergakademie Freiberg, Leipziger Strasse 29, 09596, Freiberg, Germany*

† Electronic supplementary information (ESI) available: Further details of the B3LYP/6-31G** energies of all 47 α,β-unsaturated carbonyls in their ground state and TS without and with protonation, and of the Boltzmann weighting of their principal conformers. See DOI: 10.1039/c1ob06065a

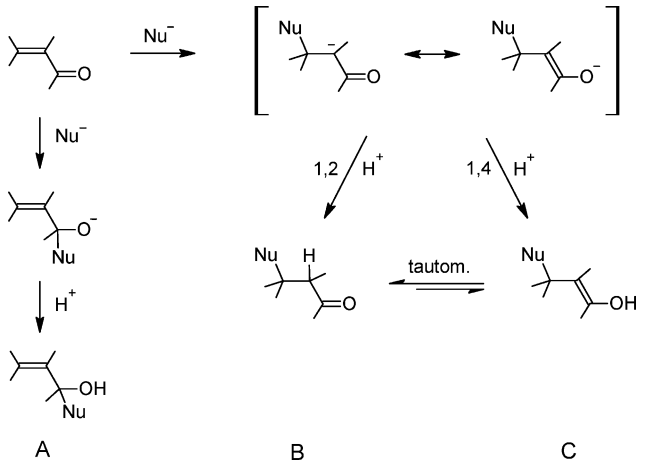

Scheme 1 Addition reactions of nucleophiles Nu^- at α,β-unsaturated carbonyl compounds. A: 1,2-carbonyl addition yielding an α-hydroxylated alkene derivative. B: 1,2-olefin addition resulting in a carbonyl derivative. C: 1,4-conjugated addition generating an enol that may tautomerize to the isomeric carbonyl compound. B and C represent two Michael-addition pathways.

1,4-conjugated reaction mechanism, passing through an enolate intermediate that after protonation tautomerizes to a ketone as final product (Scheme 1, reaction path C).

Alternative reaction pathways include a 1,2-olefin addition at the activated double bond leading directly to the ketone (Scheme 1, pathway B), and – though usually less likely for α,β-unsaturated carbonyls – a 1,2-carbonyl addition resulting in α-hydroxylated alkene derivatives (Scheme 1, pathway A). According to a recent quantum chemical analysis, the 1,2-olefin addition mechanism appears to be strongly preferred for α,β-unsaturated esters, because in this case the final tautomerization step was calculated to be energetically too unfavourable for both kinetic and thermodynamic reasons.[27] Note further that in case of strongly electron-withdrawing β-carbon substituents, the double-bond polarity may be redirected to yield substitution at the α-carbon, a pathway called anti-Michael addition.[5]

Although the Michael donor nucleophilicity is enhanced through base catalysis, one study has pointed out that acidic catalysis may yield a remarkable enhancement of the reaction rate, which has been nine orders of magnitude in case of the addition of anilines to 3-butyn-2-one.[28] In Scheme 2, both this protonated pathway and the neutral counterpart of the 1,2-olefin addition are shown including sketches of the associated 4-ring-containing transition state structures that are subject of our present study (see below).

Because the electrophilic reactivity of Michael acceptors is an important determinant of their toxicity, there is now increasing interest in its quantification through experimental[14–17,29–31] and computational[27,32–34] approaches. In this context, the tripeptide glutathione (GSH) has proven useful as model nucleophile for determining the thiol reactivity of electrophilic contaminants through their 2nd-order rate constants of reaction with GSH (k_{GSH}).[14,15]

In the present investigation, a quantum chemical approach is undertaken to predict toxicity-relevant electrophilic reactivity in terms of log k_{GSH} through transition-state energies $\Delta E^{\ddagger}$ of respective model reactions for a set of 35 α,β-unsaturated aldehydes, ketones and esters. To this end, methane thiol (CH_3SH) is used as computational surrogate for GSH, focussing on intrinsic (gas-phase) reaction barriers and a Boltzmann weighting to account for conformational degrees of freedom. For an enlarged set of 47 α,β-unsaturated carbonyls, the accordingly calculated $\Delta E^{\ddagger}$ and log k_{GSH} values are shown further to enable the prediction of their toxicity toward ciliates (48-h growth inhibition of *Tetrahymena pyriformis*) in combination with log K_{ow} (octanol/water partition coefficient), which demonstrates the feasibility of the quantum chemical approach for screening the reactive toxicity of Michael-type electrophiles.

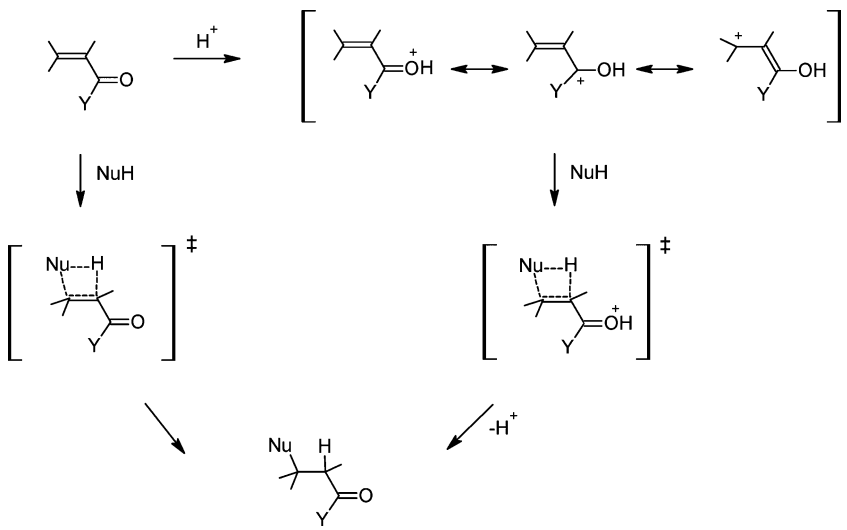

Scheme 2 Alternative pathways for the 1,2-olefin addition at α,β-unsaturated carbonyls. Left: Attack of NuH at the neutral Michael acceptor. Right: Initial protonation of the carbonyl oxygen with subsequent β-carbon attack of NuH to form a protonated ketone that is subsequently deprotonated to yield the final product. Y: H for aldehydes, R for ketones, and OR for esters.

Table 1 47 α,β-Unsaturated carbonyls covering 16 aldehydes, 12 ketones and 19 esters with information on their Michael-acceptor reactivity, hydrophobicity, and toxicity[a]

Compound	No.[b]	CAS	$\Delta E^{\ddagger}$ (kJ mol^{-1})	I_{α}	Experimental log k_{GSH} (L mol^{-1} min^{-1})	Predicted log k_{GSH} (L mol^{-1} min^{-1})	log K_{ow}	Experimental log EC_{50} (mol L^{-1})	Predicted log EC_{50} (mol L^{-1})
16 α,β-unsaturated aldehydes									
acrolein	1A	107-02-8	14.50	0	n.a.[c]	4.27	0.19	–4.87	–4.70
methylacrolein	1B	78-85-3	29.56	1	2.31	2.18	0.74	–3.45	–3.69
2-ethylacrolein	1C	992-63-4	34.21	1	1.77	1.93	1.23	–3.91	–3.77
2-butylacrolein	1D	1070-66-2	34.47	1	n.a.	1.91	2.21	–4.07	–4.16
crotonaldehyde	1E	123-73-9	60.93	0	n.a.	1.70	0.60	–3.70	–3.67
trans-2-pentenal	1F	1576-87-0	61.83	0	1.45	1.65	1.09	–3.66	–3.85
4-methyl-2-pentenal	1G	5362-56-1	66.41	0	1.03	1.39	1.51	–3.82	–3.90
2-heptenal	2A	18829-55-5	66.62	0	n.a.	1.38	2.07	–4.05	–4.13
trans-octenal	2B	2548-87-0	67.18	0	1.26	1.35	2.57	–4.20	–4.32
2-nonenal	2C	18829-56-6	67.72	0	n.a.	1.32	3.06	–4.60	–4.51
trans-2-decen-1-al	2D	3913-81-3	68.00	0	1.00	1.30	3.55	–4.85	–4.70
trans-2,*cis*-6-nonadienal	2E	557-48-2	71.46	0	1.36	1.11	2.84	–4.34	–4.32
2-methyl-2-pentenal	2F	623-36-9	73.99	1	–0.56	–0.28	1.64	–2.98	–2.91
trans-2-methyl-2-butenal	2G	497-03-0	76.39	1	–0.32	–0.42	1.15	–2.86	–2.65
2,4-dimethyl-2,6-heptadienal	3A	—	83.56	1	n.a.	–0.82	2.90	–3.08	–3.18
3-methyl-2-butenal	3B	107-86-8	92.32	0	0.23	–0.05	1.15	–3.09	–3.09
12 α,β-unsaturated ketones									
3-buten-2-one	3C	78-94-4	28.19	0	n.a.	3.51	0.41	–4.51	–4.63
1-penten-3-one	3D	1629-60-3	37.31	0	3.10	3.01	0.90	–4.52	–4.51
1-hexen-3-one	3E	1629-60-3	37.96	0	3.07	2.97	1.39	–4.66	–4.66
1-octen-3-one	3F	4312-99-6	39.79	0	3.03	2.87	2.37	–4.92	–4.95
3-penten-2-one	3G	625-33-2	67.51	0	1.43	1.33	0.82	–3.54	–3.52
3-hepten-2-one	4A	1119-44-4	70.24	0	1.10	1.18	1.80	–3.70	–3.77
3-octen-2-one	4B	1669-44-9	71.48	0	1.06	1.11	2.29	–3.74	–3.90
3-nonen-2-one	4C	14309-57-0	71.95	0	1.03	1.08	2.79	–3.98	–4.06
4-hexen-3-one	4D	625-33-2	75.40	0	1.38	0.89	1.31	–3.93	–3.43
2-octen-4-one	4E	4643-27-0	76.66	0	1.42	0.82	2.29	–4.01	–3.74
3-methyl-3-penten-2-one	4F	565-62-8	79.71	1	–0.11	–0.60	1.37	–2.66	–2.66
4-methyl-3-penten-2-one	4G	141-79-7	99.35	0	–0.68	–0.44	1.37	–2.36	–2.69
19 α,β-unsaturated esters									
methyl acrylate	5A	96-33-3	64.40	0	1.06	1.50	0.73	–3.55	–3.68
propargyl acrylate	5B	10477-47-1	65.30	0	1.71	1.45	0.94	–4.06	–3.71
2-hydroxyethyl acrylate	5C	818-61-1	68.17	0	n.a.	1.29	–0.25	–3.69	–3.29
ethyl acrylate	5D	140-88-5	70.01	0	1.03	1.19	1.22	–3.52	–3.62
propyl acrylate	5E	925-60-0	71.09	0	1.01	1.13	1.71	–3.53	–3.71
butyl acrylate	5F	141-32-2	71.94	0	0.93	1.08	2.20	–3.52	–3.81
allyl acrylate	5G	999-55-3	72.21	0	1.29	1.07	1.57	–3.68	–3.63
tert-butyl acrylate	6A	1663-39-4	81.47	0	0.40	0.55	2.09	–3.27	–3.45
propargyl methacrylate	6B	13861-22-8	82.03	1	–0.66	–0.73	1.49	–2.63	–2.27
methyl methacrylate	6C	80-62-6	82.73	1	–1.14	–0.77	1.28	–1.78	–2.19
2-hydroxyethyl methacrylate	6D	868-77-9	86.47	1	n.a.	–0.98	0.30	–1.92	–1.80
ethyl methacrylate	6E	97-63-2	87.73	1	–1.24	–1.05	1.77	–2.07	–2.14
vinyl crotonate	6F	14891-06-4	98.33	0	n.a.	–0.38	1.50	–2.85	–2.71
methyl crotonate	6G	623-43-8	99.11	0	–0.79	–0.43	1.44	–2.08	–2.66
methyl *trans*-2-octenoate	7A	7367-81-9	100.04	0	–0.11	–0.48	3.10	–3.76	–3.07
ethyl *trans*-crotonate	7B	623-70-1	103.16	0	–0.79	–0.65	1.63	–2.24	–2.57
n-butyl crotonate	7C	7299-91-4	104.86	0	n.a.	–0.74	2.61	–2.84	–2.77
methyl tiglate	7D	6622-76-0	111.51	1	–2.15	–2.37	1.69	–2.38	–1.30
methyl 3,3-dimethylacrylate	7E	924-50-5	124.71	0	n.a.	–1.85	1.69	–1.94	–1.84

[a] The compound properties are: $\Delta E^{\ddagger}$ (kJ mol^{-1}) = B3LYP/6-31G** conformer-averaged (Boltzmann-weighted) reaction barrier of the protonated pathway Michael addition of CH_3SH; I_{α} = indicator variable discriminating between the absence ($I_{\alpha} = 0$) and presence ($I_{\alpha} = 1$) of a substituent at the α-carbon of the Michael acceptor; k_{GSH} (L mol^{-1} min^{-1}) = 2nd-order rate constant of reaction with glutathione (GSH), with experimental values[14,15,32] and predicted values from the final two-variable regression model of Table 2 employing $\Delta E^{\ddagger}$ and I_{α} that was calibrated with the subset of 35 α,β-unsaturated carbonyls with experimental values ($r^2 = 0.955$, rms = 0.263, see Table 2); log K_{ow} = calculated logarithmic octanol/water partition coefficient;[43] experimental log EC_{50} (48-h 50% growth inhibition of *Tetrahymena pyriformis*) values,[13,15,37–42] and predicted values according to the three regression models of Table 5 employing log K_{ow}, $\Delta E^{\ddagger}$ and I_{α} calibrated for 16 aldehydes, 12 ketones and 18 esters (methyl tiglate excluded). [b] The number scheme refers to Scheme 3 where all associated chemical structures are shown. [c] No experimental value available.

Results and discussion

In Table 1, all 47 compounds of the present study are listed with Boltzmann-weighted $\Delta E^{\ddagger}$ (see below) and further calculated and experimental properties (for details about the individual conformer energies, see the ESI†). The associated chemical structures are shown in Scheme 3.

All three compound classes contain structures without α-C and β-C substitution (*e.g.* 1A, acrolein; 3C 3-buten-2-one; 5A, methyl acrylate), and derivatives with α-C (*e.g.* 1B, methyl

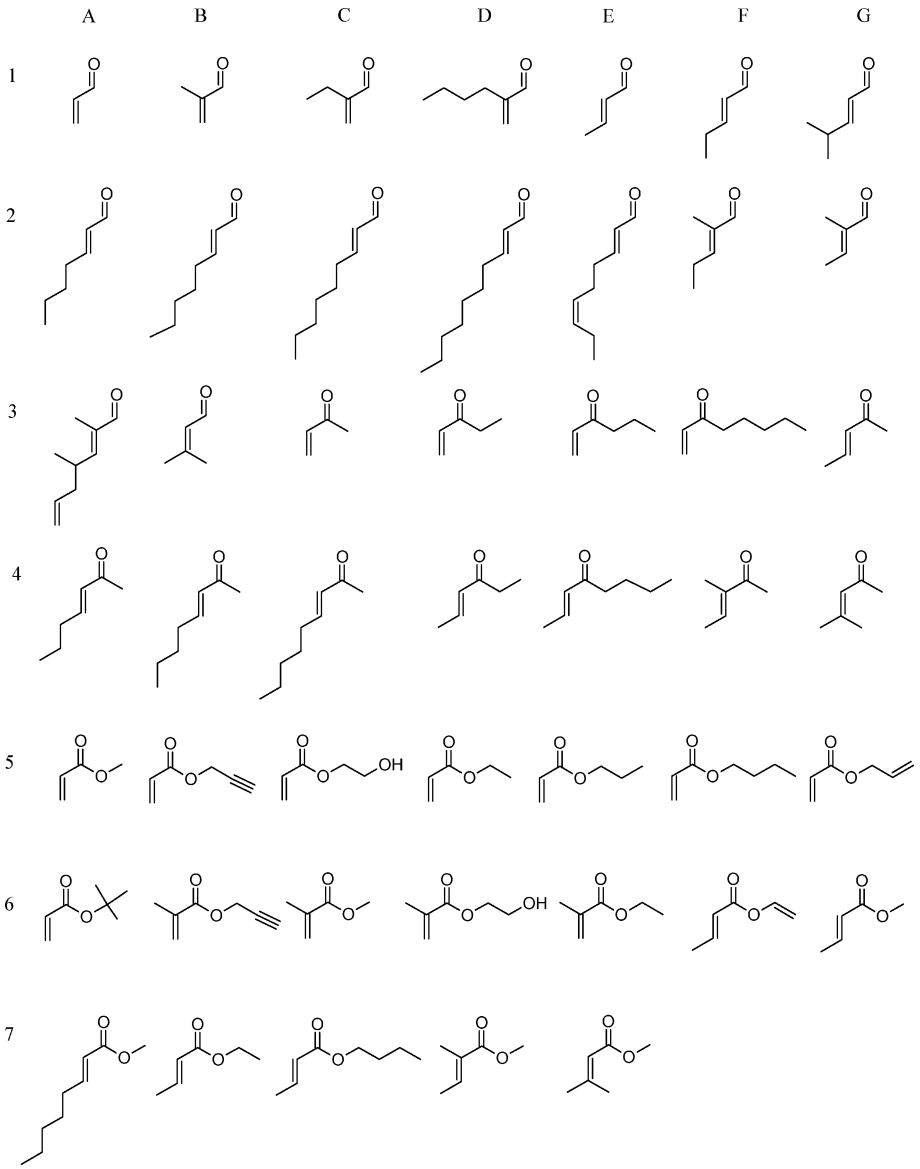

Scheme 3 Chemical structures of the compound set of 47 α,β-unsaturated carbonyls covering 16 aldehydes (1A-3B), 12 ketones (3C-4G) and 19 esters (5A-7*E*) listed in Table 1 together with their names, CAS numbers and further molecular properties.

acrolein), β-C (*e.g.* 1E, crotonaldehyde) or both α-C and β-C substituents (*e.g.* 2G, 2-methyl-2-butenal; 4F, 3-methyl-3-penten-2-one; 7D, methyl tiglate). As will be discussed in more detail below, α-C and β-C substitution have distinct effects on the Michael acceptor reactivity, and thus provide opportunity to test the suitability of calculation schemes for their prediction.

For the subset of 35 Michael acceptors with experimental second-order rate constants of their reaction with GSH,[14,15,32] the respective reactivity varies by 4.5 orders of magnitude (log k_{GSH} from −2.15 (7D) to 2.31 (3D, 1-penten-3-one)). Interestingly, two ketones without experimental rate constants are predicted to be still more reactive than 1-penten-3-one: For acrolein (1A) and 3-buten-2-one (3C), our calculations yield log k_{GSH} values of 4.27 and 3.51, respectively (Table 1).

Energy profile of the two reaction pathways

As outlined above, the Michael addition of the model nucleophile methane thiol (CH_3SH) at the α,β-unsaturated carbonyl may proceed through initial attack at the β-carbon (Scheme 2, left), or alternatively through initial protonation of the carbonyl oxygen (Scheme 2, top and right). The associated general energy profiles subject to present computational analysis are summarized in Scheme 4. For the pathway without protonation, reaction of the Michael acceptor A (in our case: α,β-unsaturated carbonyl) with nucleophile B (in our case: CH_3SH) yields a neutral transition state (TS) $[AB]^{‡}$ with an associated energy increase $\Delta E^{‡}$, leading to the final product P, the ketone.

Initial protonation of the Michael acceptor A to yield HA^+ is accompanied by an energy decrease of 841–944 kJ mol^{-1} (when considering the model reaction in the gas phase at the

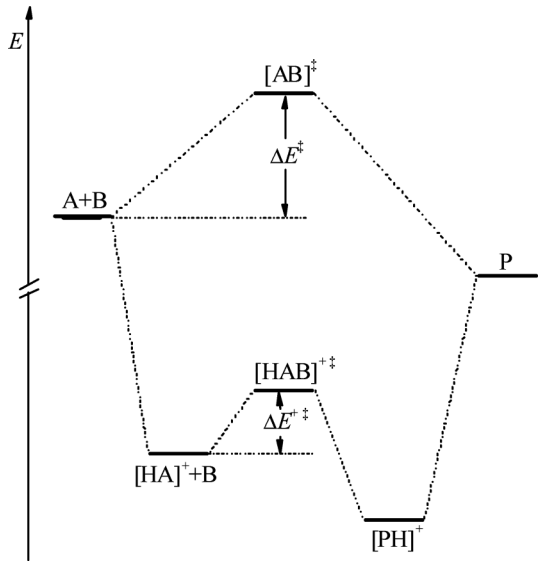

Scheme 4 Qualitative energy diagram for the neutral and protonated reaction pathway of the nucleophilic 1,2-olefin addition of nucleophile B (methane thiol, CH_3SH) at α,β-unsaturated carbonyls A, leading to a ketone as final product P. Initial protonation of A yields an energetically much lower reactant pair $[HA]^+$ + B as compared to A + B. Note the difference between the reaction barriers $\Delta E^{\ddagger}$ and $\Delta E^{+\ddagger}$ of the neutral and protonated transition states, $[AB]^{\ddagger}$ and $[HAB]^{+\ddagger}$, respectively.

B3LYP/6-31G** level). The subsequent reaction proceeds through a positively charged TS, $[HAB]^{+\ddagger}$, as rate-determining step, forming the protonated product PH^+ (the protonated 1,2-adduct). Subsequent deprotonation leads to the ketone as final product P. Both reaction pathways contain several elementary steps connecting different geometric arrangements of the molecular species, and in both cases formation of the first TS (the only TS referred to in both Schemes 2 and 4) is considered rate-determining for the overall Michael addition.

Concerning the TS energy barriers, $\Delta E^{\ddagger}$ (kJ mol^{-1}) ranges from 173.7 to 206.0 for $[AB]^{\ddagger}$ (neutral pathway), and from 5.1 to 126.9 for $[HAB]^{+\ddagger}$ (protonated pathway) when taking into account conformational degrees of freedom (see below). While the lower energy barriers obtained for the protonated pathway reflect the increased electrophilicity of the β-carbon as expected from considering the mesomeric stabilization C═C–C═OH$^+$ ↔ C$^+$–C═C–OH, their substantially larger variation as compared to the neutral reaction pathway (121.8 *vs.* 32.3 kJ mol^{-1}) indicates a correspondingly larger sensitivity on structural features of the Michael acceptor. Interestingly, the variation in reaction energy is also smaller for the neutral pathway (57.2 kJ mol^{-1}: from −86.9 to −29.7 kJ mol^{-1} for E(P) − E(A + B), see Scheme 4) than after initial Michael acceptor protonation (125.0 kJ mol^{-1}: from −108.6 to 16.4 kJ mol^{-1} for E([PH]$^+$). Note that the individual energies of all relevant molecular species are listed in the ESI.†

Boltzmann distribution of reactant conformers

Except for CH_3SH, all molecular structures under analysis have several non-equivalent local minima as ground-state conformations, which are populated at a given temperature according to a Boltzmann distribution. The latter has been taken into account to derive effective (Boltzmann-weighted) reaction barriers $\Delta E^{\ddagger}$, considering the general situation as outlined in Scheme 5.

As illustrated in this scheme, internal rotation of Michael acceptor A around the single bond connecting both double bonds, C_β═C_α–C═O, leads to two different conformations representing the s-*cis* and s-*trans* orientation called A_c and A_t, respectively. Each of these two conformers can be protonated in a synperiplanar or antiperiplanar orientation, resulting in the four conformers HA^+_{cs} (s-*cis*, synperiplanar), HA^+_{ca} (s-*cis*, antiperiplanar), HA^+_{ts} (s-*trans*, synperiplanar), and HA^+_{ta} (s-*trans*, antiperiplanar; see Scheme 5). It follows that for the geometry of the carbonyl reactant, (at least) two conformers may be relevant for the neutral reaction pathway, and (at least) four for the pathway involving initial protonation.

Assuming a Boltzmann distribution of the conformers of a given molecular species, the fraction of each conformer i, x_i, can be expressed as

$$x_i = \frac{\exp\left(-\frac{\Delta G_i}{RT}\right)}{\sum_k \exp\left(-\frac{\Delta G_k}{RT}\right)} \quad (1)$$

where ΔG_i represents the free energy difference between conformer i and the conformer with the lowest free energy, R the gas constant, and T the absolute temperature (that was set to 298.15 K). These mole fractions x_i were applied as weighting factors for the corresponding reaction barriers in all cases where different reactant ground-state conformations were available for a given TS geometry. The relevant formula is

$$\Delta E^{\ddagger} = -RT \ln \sum_i x_i \exp\left[-\frac{\Delta E_i^{\ddagger}}{RT}\right] \quad (2)$$

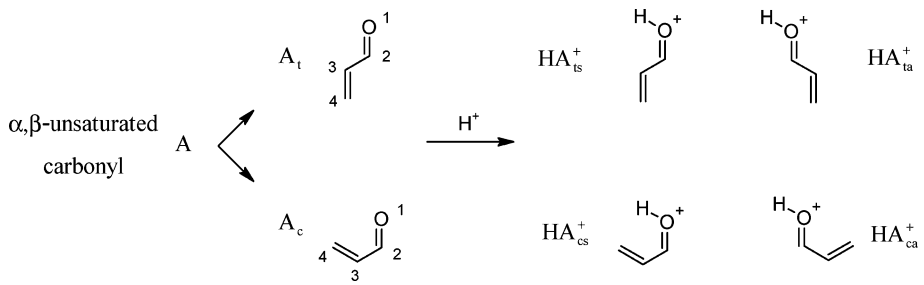

Scheme 5 Michael-acceptor (A) conformations involved in the addition of a nucleophile for both the neutral and protonated reaction pathway. A_s and A_t represent the s-*cis* and s-*trans* conformations of the neutral Michael acceptor A, while protonation at the carbonyl oxygen leads to the four conformations HA^+_{cs} (s-*cis*, synperiplanar), HA^+_{ca} (s-*cis*, antiperiplanar), HA^+_{ts} (s-*trans*, synperiplanar), and HA^+_{ta} (s-*trans*, antiperiplanar), respectively.

where $\Delta E_i^{\ddagger}$ denotes the difference in reaction barrier between conformer i and the conformer with the lowest free energy. If, however, there were several TS conformations associated with only one reactant conformer, only the lowest-energy TS conformation (and thus the lowest-possible reaction barrier) was taken into account.

Concerning the example of Scheme 5, two conformers would be considered for evaluating the mole fractions of the carbonyl reactant for the neutral reaction pathway, and four conformers for the pathway involving protonation. Interestingly, in all minimum-energy conformers the β-carbon reaction site has a near-planar geometry.

For the individual conformations (*i.e.* before Boltzmann weighting), the calculated activation energies $\Delta E^{\ddagger}$ (kJ mol^{-1}) of the neutral reaction pathway are 180.6–206.0 (aldehydes), 173.7–192.2 (ketones) and 180.9–202.6 (esters), respectively. For the reaction starting from the protonated Michael acceptor, conformer-specific $\Delta E^{\ddagger}$ (kJ mol^{-1}) is 5.1–94.9 (aldehydes), 26.6–107.6 (ketones) and 63.8–126.9 (esters), respectively. It shows that upon protonation, the following two features emerge: First, the order of the calculated reactivity range changes from ketones > aldehydes ≈ esters to aldehydes > ketones > esters (keeping in mind that these ranges are driven by the particular selection of compounds considered). Second (and as already mentioned), $\Delta E^{\ddagger}$ becomes significantly more sensitive for the particular reactant structure.

When confining the comparison to the subset of 35 compounds with experimentally determined reaction rate constants, the experimental (predicted) log k_{GSH} range is –0.56 to 2.31 (–0.41 to 2.18) for the 10 aldehydes, –0.68 to 3.10 (–0.60 to 3.01) for the 11 ketones, and –2.15 to 1.71 (–2.37 to 1.45) for the 14 esters. It shows that the order of the experimentally observed[14,15,32] Michael-acceptor reactivity range for the 35 α,β-unsaturated carbonyls, ketones > aldehydes > esters, is reproduced by our computational approach as discussed in more detail below.

Transition-state characteristics

All optimized Michael acceptor structures have a nearly planar geometry at the β-carbon as primary reaction site. Nucleophilic attack by CH_3SH can occur from above or below this plane. In the TS, the CH_3SH sulphur is already pretty close to the β-C, and the thiol H (called H_S because of its initial attachment to S) approaches the α-carbon, forming a 4-membered ring (see Scheme 2).

At this saddle point of the reaction, the bond-forming S–C_β distance is 2.51 to 2.82 Å for the neutral reaction path and 1.87 to 1.96 Å for the protonated reaction path (as compared to optimized product S–C_β distances of 1.83 to 1.88 Å), and the other bond-forming H_S–C_α distance is 1.22 to 1.37 Å for the neutral reaction path and 1.39 to 1.67 Å for the protonated reaction path (as compared to optimized product H_S–C_α distances of 1.09 to 1.11 Å), respectively. It follows that for the 1,2-olefin addition of CH_3SH at protonated α,β-unsaturated carbonyls as one possible pathway of the Michael addition, the TS is late concerning the (almost completed) S–C_β bond formation, but early concerning the H_S–C_α bond formation. The TS of the neutral reaction path shows reversed characteristics, being early concerning the S–C_β bond formation, and late concerning the H_S–C_α bond formation.

With regard to the methyl thiolate (CH_3S^-) addition to acrolein computed with inclusion of solvation, previous studies found the S–C_β distance in the TS to be 2.4 Å.[27] According to our present results, the respective TS is geometrically closer to the ones obtained for the neutral reaction path, and can therefore be considered early concerning the S–C_β bond formation. The same pattern was observed for the reaction of methyl acrylate (methyl propenoate) with deprotonated β-mercaptopropionic acid, where an S–C_β distance of 2.5 Å had been found in the TS.[35] These findings underline the distinctive features of the protonated reaction path.

The TS geometry is illustrated in Scheme 6, showing the 4-membered ring involving thiol sulphur and hydrogen of CH_3SH and the β- and α-carbon of the Michael-acceptor carbonyl (left), and the dihedral angle θ as further geometric variable of the TS (right).

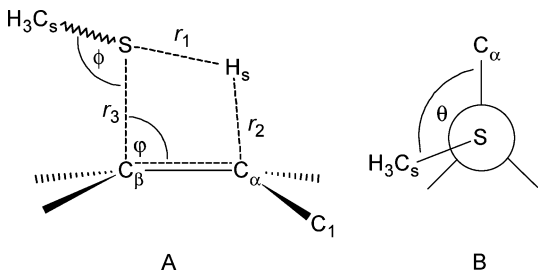

Scheme 6 Geometric coordinates determining the transition state (TS) of the 1,2-olefin addition of the nucleophile CH_3SH at α,β-unsaturated carbonyls. A: 4-ring TS showing three atom-atom distances r_1 (S–H), r_2 (SH–C_α) and r_3 (HS–C_β) as well as the bond angles φ (S–C_α–C_β) and ϕ (H_3C–S–C_β). B: View along the S–C_β bond illustrating the dihedral angle θ.

Frequency analysis of the TS reveals that the imaginary frequency corresponds mainly to the further H_S movement toward C_α. Accordingly, the rate-determining step of the 1,2-olefin addition of CH_3SH at α,β-unsaturated carbonyls – as modelled in the gas phase – is governed by the proton transfer between thiol H and α-C. While the overall addition reaction proceeds in a concerted manner through a 4-membered ring as TS as shown in Scheme 6, the S–C_β bond formation precedes the H_S–C_α bond formation.

Due to the planarity of the reaction centre, the computational reaction analysis could be confined to the attack from only one side, thus reducing the number of TS geometries to be investigated. With this approach, one TS was identified for both the s-*cis* and s-*trans* reactant conformer (Scheme 5) in the neutral reaction pathway. Concerning the protonated pathway, each of the four principal conformers (s-*cis* synperiplanar, s-*cis* antiperiplanar, s-*trans* synperiplanar and s-*trans* antiperiplanar, see Scheme 5) yielded two non-degenerated TS structures, rendering a total of 470 TS geometries optimized at the DFT/6-31G** level.

Predicting Michael-acceptor reactivity from reaction barrier $\Delta E^{\ddagger}$

For the subset of 35 α,β-unsaturated carbonyls with experimental log k_{GSH} values,[14,15,32] the suitability of the quantum chemically calculated energy barrier of their reaction with the model nucleophile CH_3SH, $\Delta E^{\ddagger}$, for predicting log k_{GSH} could be explored.

Initial regression analysis of log k_{GSH} *vs.* $\Delta E^{\ddagger}$ yielded two major findings:

First, inspection of the data distribution revealed a clear separation between compounds without and with α-substitution, where the α-substituted compounds showed systematically too high predicted log k_{GSH} values because of correspondingly too low reaction barriers. This finding indicates that for the solution-phase reaction of Michael acceptors with GSH, α-C substitution reduces their reactivity much more than for the corresponding gas-phase 1,2-olefin addition pathway analyzed here (with CH_3SH as surrogate for GSH).

Possible explanations are that the α-substituent effect differs systematically between the 1,2-olefin addition and the 1,4-conjugated addition of Michael acceptors, that bulk solvation affects specifically the impact of α-carbon substitution, and that the solution-phase reaction involves a catalytic micro-solvation of the α-carbon by water (as discussed earlier for the case of the NH_3 addition to α,β-unsaturated carbonyls)[36] that is not captured in a computational gas-phase description. Note, however, that inclusion of aqueous micro-solvation would require a judicious choice of the number of water molecules required, keeping in mind that the latter appears to affect the solvation energy in a non-monotonous way.[27] For the time being, the described and essentially incremental α-substituent effect can be empirically accounted for through introduction of an indicator variable I_{α}, being 1 for α-substituted Michael acceptors, and 0 otherwise.

Second, comparison between the log k_{GSH} regression results for the neutral and protonated pathway shows that the latter yields significantly superior statistics ($r^2 = 0.20$ *vs.* 0.96 for 9 α-substituted compounds, and $r^2 = 0.01$ *vs.* 0.93 for 26 α-H compounds). On the one hand, this appears to support the view that the Michael addition involves initial protonation at the carbonyl oxygen, thus enhancing the electrophilicity of the β-carbon for the subsequent attack by the nucleophile[28] as discussed above. On the other hand, this result may be driven by our focus on intrinsic reaction barriers without considering bulk or catalytic solvation effects on the Michael-acceptor reactivity (see however below). In any case, the results demonstrate that the neutral pathway TS energies – despite Boltzmann-weighting of the conformational flexibility – do not inform properly about the order of the Michael-acceptor reactivity toward GSH, while consideration of initial protonation of the carbonyl oxygen yields high correlations between calculated $\Delta E^{\ddagger}$ and experimental log k_{GSH}.

In Table 2, the regression results are summarized for the protonated pathway. While the subsets without and with α-substitution yield similar statistics ($r^2 = 0.96$ and 0.93, respectively) with very similar $\Delta E^{\ddagger}$ regression coefficients (–0.0544 *vs.* –0.0564), their intercepts differ significantly (3.74 *vs.* 5.14), indicating a respective shift in log k_{GSH} concerning the $\Delta E^{\ddagger}$ scale. For the combined set of 35 compounds, introduction of the above-described indicator variable I_{α} increases r^2 from 0.76 to 0.96 (and decreases rms from 0.61 to 0.26 log units). Thus, employing both $\Delta E^{\ddagger}$ and I_{α} (that serves as empirical α-substitution effect correction) provides a way for predicting the Michael-acceptor reactivity of aldehydes, ketones and esters in terms of log k_{GSH}. The respective data distribution is shown in Fig. 1. Note further that the log k_{GSH} regression rms error of around 0.26 log units when differentiating between α-H and α-substitution is larger than the experimental error of below 0.07 log units for all 35 compounds measured in our lab.[14,15,32]

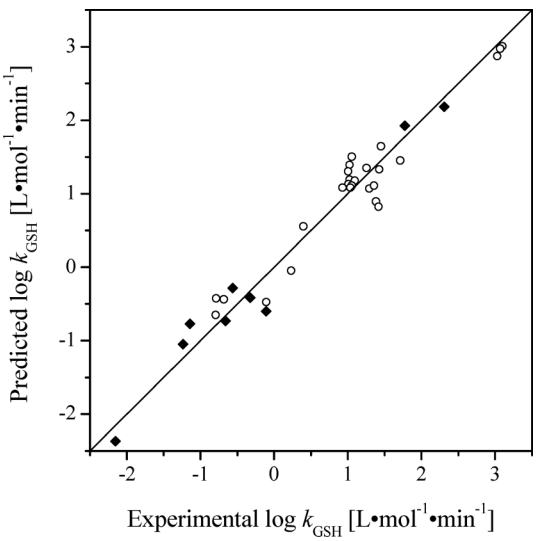

Fig. 1 Calculated *vs.* experimental Michael-acceptor reactivity in terms of log k_{GSH} (L mol^{-1} min^{-1}) for 35 α,β-unsaturated carbonyl compounds ($r^2 = 0.96$, rms = 0.26, $q^2_{cv} = 0.95$, $rms_{cv} = 0.29$, $F_{2,32} = 337$; for the data see Table 1). Solid diamonds and open circles represent derivatives with and without α-C substitution, respectively.

When omitting the Boltzmann weighting according to eqn (1) and (2) and taking only the minimum-energy reaction barrier (see

Table 2 Regression models for predicting the logarithmic rate constant of reaction with glutathione, log k_{GSH}, of α,β-unsaturated aldehydes, esters and ketones from calculated Michael-addition reaction barriers[a]

Compound type	*n*	*a*	*b*	*c*	r^2	rms	q^2_{cv}	rms_{cv}	*F*
Log k_{GSH} (L mol^{-1} min^{-1}) = $a \cdot \Delta E^{\ddagger}$ (kJ mol^{-1}) + $b \cdot I_{\alpha} + c$									
α-substituted	9	–0.0544 (± 0.0040)	—	3.74 (± 0.31)	0.964	0.255	0.957	0.333	187.7
Not α-substituted	26	–0.0564 (± 0.0032)	—	5.14 (± 0.24)	0.929	0.265	0.924	0.289	313.5
All	35	–0.0562 (± 0.0055)	—	4.80 (± 0.41)	0.758	0.608	0.738	0.660	103.3
All	35	–0.0555 (± 0.0024)	–1.25 (± 0.11)	5.08 (± 0.18)	0.955	0.263	0.950	0.289	337.2

[a] The compounds and associated experimental log k_{GSH} values[14,15,32] are listed in Table 1. The parameters are: *n* = number of compounds; *a*, *b*, *c* = regression parameters; $\Delta E^{\ddagger}$ (kJ mol^{-1}) = B3LYP/6-31G** conformer-averaged protonated pathway reaction barrier of the Michael addition of CH_3SH; I_{α} = indicator variable discriminating between the absence ($I_{\alpha} = 0$) and presence ($I_{\alpha} = 1$) of a substituent at the α-carbon of the Michael acceptor; r^2 = squared correlation coefficient, q^2_{cv} = squared predictive correlation coefficient estimated through leave-one-out cross validation,[48] rms = root-mean-square error, rms_{cv} = cross-validated root-mean-square error, *F* = *F*-test value referring to one ($F_{1,n-2}$) or two ($F_{2,n-3}$) regression variables.

Scheme 4), r^2 decreases from 0.96 to 0.91, and rms increases from 0.22 to 0.38, which is similar to taking only the minimum-energy barrier of the minimum-energy conformer (r^2 = 0.92 and rms = 0.37; detailed results not shown). For the four conformations of the protonated pathway, the corresponding separate statistics are r^2 = 0.87 and rms = 0.46 (s-*cis* synperiplanar), r^2 = 0.91 and rms = 0.38 (s-*cis* antiperiplanar), r^2 = 0.87 and rms = 0.46 (s-*trans* synperiplanar), and r^2 = 0.87 and rms = 0.47 (s-*trans* antiperiplanar), respectively. These results demonstrate the relevance of taking into account the conformational distribution, keeping in mind that the level of computation feasible is significantly more limited for multi-conformer approaches (in our case: *ca.* 470 TS geometry optimizations as mentioned above) than for minimum-energy conformer calculation schemes.

Employing $\Delta G^{\ddagger}$ (at 25 °C and 1 atm) instead of $\Delta E^{\ddagger}$ yields inferior but still good statistics, with r^2 values of 0.939, 0.906 and 0.936 for the subsets of α-substituted and α-H compounds and their combination with inclusion of I_{α}, and associated rms errors of 0.378, 0.317 and 0.327, respectively (for details see ESI†). Note, however, that the harmonic oscillator approximation used for calculating $\Delta G^{\ddagger}$ may yield substantial errors for soft vibrational modes, which requires particular attention when quantifying TS frequencies.

In order to test the potential impact of bulk aqueous solvation on the α-substitution issue, single-point calculations involving a polarisable continuum model (PCM) have been performed (see Table 3). Again, separate regressions for α-substituted and α-H compounds yield similar $\Delta E^{\ddagger}$ regression coefficients (–0.0685 *vs.* –0.0616). Interestingly, the difference in intercept between both subsets has reduced substantially (from 1.4 to 0.4 log units) and is now smaller than the individual regression coefficient errors that in turn are significantly larger than for the corresponding gas-phase regression equations (α-substituted: 1.3 *vs.* 0.31, α-H: 0.67 *vs.* 0.24; see Tables 2 and 3). As with the gas-phase calculations, the corresponding neutral pathway statistics are very poor (r^2 = 0.3, 0.05 and 0.04 for α-substituted, α-H and all 35 compounds). Overall, the PCM results support the view that the α-effect observed for the gas-phase calculations is at least partly driven by the lack of solvation. At the same time, the PCM statistics are significantly inferior to the gas-phase counterparts (r^2 up to 0.85 *vs.* 0.96, rms down to 0.50 *vs.* 0.26), possibly because of limitations involved in the PCM approximation.

In a recent study of the reaction of CH_3SH with 11 (mostly different) Michael acceptors, both micro-solvation through explicit water molecules and a continuum solvation model for incorporating bulk effects were taken into account.[27] An important result was that the reaction barriers were strongly dependent on the number of solvent molecules included in the calculations (s.a.). Moreover, it had been pointed out earlier that the calculated reaction barrier is substantially reduced when incorporating a water molecule as catalyst for the proton transfer from the nucleophile to the Michael acceptor, again with inclusion of a continuum model for the additional bulk solvation.[36] However, in that study the experimentally known reactivity order acrylonitrile < acrylic acid < acrolein was reproduced only for the 1,4-conjugated addition mechanism, and not for the alternative 1,2-olefin addition pathway. This contrasts with our present gas-phase results, showing a very good correlation of calculated reaction barriers of the latter mechanism with observed reaction rate constants for a series of 35 α,β-unsaturated carbonyls when considering the protonated pathway and taking into account Boltzmann-weighted conformer energies.

In another recent investigation, transition-state calculations were used for predicting log k_{GSH} for 22 Michael-acceptor aldehydes, esters and ketones.[34] Regression models employing three variables were derived for gas-phase calculations (r^2 = 0.84), and for continuum-solvation calculations without (r^2 up to 0.90) and with additional micro-solvation through two water molecules (r^2 up to 0.87). Major conclusions were that both the energy of the enol intermediate relative to the Michael-acceptor energy and the (calculated) geometric accessibility of the β-carbon were important, and that the keto-enol tautomerism was not rate-determining (the latter of which contrasts with the Paasche *et al.*[27] results concerning esters). Interestingly, the forward reaction barrier alone as well as its combination with the geometric accessibility of the β-carbon were only poor predictors for log k_{GSH} (r^2 = 0.004 and 0.51, respectively). Only additional inclusion of the backward reaction barrier from the enol intermediate resulted in good statistics.

From the viewpoint of these earlier computational investigations, our present approach differs in the following major issues: First, we explored the 1,2-olefin addition as possible reaction pathway (keeping in mind that the available experimental data do not inform about the actual or prevalent reaction mechanism). Second, we considered both the neutral and protonated form of

Table 3 Regression models for predicting the logarithmic rate constant of reaction with glutathione, log k_{GSH}, of α,β-unsaturated aldehydes, esters and ketones from calculated Michael-addition reaction barriers in simulated aqueous solution[a]

Compound type	*n*	*a*	*b*	*c*	r^2	rms	q^2_{cv}	rms_{cv}	*F*
Log k_{GSH} (L mol^{-1} min^{-1}) = $a \cdot \Delta E^{\ddagger}$ (kJ mol^{-1}) + $b \cdot I_{\alpha} + c$									
α-substituted	9	–0.0686 (± 0.012)	—	7.31 (± 1.3)	0.821	0.646	0.792	0.732	32
Not α-substituted	26	–0.0616 (± 0.006)	—	7.72 (± 0.67)	0.805	0.455	0.793	0.478	99
All	35	–0.0661 (± 0.008)	—	7.90 (± 0.86)	0.680	0.720	0.667	0.745	70
All	35	–0.0640 (± 0.005)	–1.17 ± (0.19)	7.96 (± 0.60)	0.850	0.500	0.831	0.530	91

[a] The parameters are: *n* = number of compounds; *a*, *b*, *c* = regression parameters; $\Delta E^{\ddagger}$ (kJ mol^{-1}) = PCM-B3LYP/6-31G**//B3LYP/6-31G** (using UAHF radii) conformer-averaged protonated pathway reaction barrier of the Michael addition of CH_3SH; I_{α} = indicator variable discriminating between the absence (I_{α} = 0) and presence (I_{α} = 1) of a substituent at the α-carbon of the Michael acceptor; r^2 = squared correlation coefficient, q^2_{cv} = squared predictive correlation coefficient estimated through leave-one-out cross validation,[48] rms = root-mean-square error, rms_{cv} = cross-validated root-mean-square error, *F* = *F*-test value referring to one ($F_{1,n-2}$) or two ($F_{2,n-3}$) regression variables.

the Michael acceptors. The reasoning behind this is as follows: Because the carbonyl oxygen is solvated under experimental reaction conditions and thus H-bonded to (at least) one positively polarized water hydrogen atom that could be represented as $R_2C{=}O\cdots H^{\delta+}{-}O^{\delta-}H$, its protonation at the carbonyl oxygen according to $R_2C{=}OH^+$ may incorporate some solution-phase characteristics into the calculation scheme without taking water molecules into account. Third, our computational analysis focuses on intrinsic reaction barriers as calculated in the gas phase, but takes into account conformational degrees of freedom through calculating Boltzmann-weighted $\Delta E^{\ddagger}$ values.

Despite all approximations involved (including the replacement of GSH by the model nucleophile CH_3SH), the present approach yields prediction statistics for log k_{GSH} significantly superior to all previous investigations, and for a substantial data set size with 35 Michael acceptors. For future investigations into the role of micro-solvation and its possible impact on α-substitution, a possible challenge is the determination of the adequate number of solvating water molecules, keeping in mind the observed substantial variation in calculated solvation effects with the size of the micro-solvation shell as reported earlier.[27]

Reactivity variation across isomeric Michael acceptors

Comparison of log k_{GSH} of isomeric Michael acceptors provides insight into its dependence on molecular structure, and into the scope and limitation of $\Delta E^{\ddagger}$ in reproducing log k_{GSH} differences. Table 1 contains four C_5-aldehydes with log k_{GSH} covering two units (2-ethyl acrolein, 1C: 1.77; 2-pentenal, 1F: 1.45; 3-methyl-2-butenal, 3B: 0.23; 2-methyl-2-butenal, 2G: –0.32), and two C_5-ketones (1-penten-3-one, 3D: 3.10; 3-penten-2-one, 3G: 1.43). The latter include 1-penten-3-one as by far most reactive C_5 isomer, which is reflected by one of the overall lowest $\Delta E^{\ddagger}$ values (37.3 kJ mol^{-1}, corresponding to a predicted log k_{GSH} of 3.01; see Table 1). While both this ketone and the isomeric aldehyde 2-ethyl acrolein have an unsubstituted β-carbon, the α-carbon is substituted only for the latter, explaining its reduced Michael-acceptor reactivity by a factor of *ca.* 20. For a yet unknown reason (see above), this α-substitution effect is not reproduced on the intrinsic reaction barrier scale; inclusion of I_α converts the (too low) $\Delta E^{\ddagger}$ value (34.2 kJ mol^{-1}) to a predicted log k_{GSH} (1.93) close to its experimental value.

Both 2-pentenal (1F, C_5-aldehyde) and 3-penten-2-one (3G, C_5-ketone) have mono-substituted α- and β-carbons, and indeed yield very similar reactivities toward GSH (log k_{GSH} 1.45 *vs.* 1.43), which is reasonably well reproduced through their Boltzmann-weighted $\Delta E^{\ddagger}$ (61.8 *vs.* 67.5 kJ mol^{-1}) and accordingly predicted log k_{GSH} values (1.65 *vs.* 1.33).

In contrast to the α-substitution effect, the impact of β-substitution on experimental log k_{GSH} is well reflected in the calculated $\Delta E^{\ddagger}$ values. This is illustrated with the subgroup of two C_5-aldehydes and two C_5-ketones (see above) without α-substitution, within which the decrease in experimental log k_{GSH} from 3.10 to –0.23 is well reflected by a corresponding increase of $\Delta E^{\ddagger}$ from 37.3 to 92.3 kJ mol^{-1} (see Table 1). While both 2-pentenal (1F) and 3-penten-2-one (3G) are singly β-substituted and similarly reactive (s.a.), the latter compound is 47-fold less reactive than 1-penten-3-one (3D) that in turn has an unsubstituted β-carbon; this experimentally observed decrease in reactivity is also reflected by their calculated $\Delta E^{\ddagger}$ values (67.5 *vs.* 37.3 kJ mol^{-1}). Among these four C_5 isomers, 3-methyl-2-butenal (3B) is the only compound with two substituents at β-C, and shows both the smallest log k_{GSH} (–0.32) and the largest $\Delta E^{\ddagger}$ (92.3 kJ mol^{-1}).

A further example is given by the two C_6-isomers 4-methyl-2-pentenal (1G) and 4-methyl-3-penten-2-one (4G), both of which have no α-substituent. The former with one β-substituent is much more reactive than the latter with two β-substituents (log k_{GSH} 1.03 *vs.* –0.68), which is also seen by their substantial difference in calculated $\Delta E^{\ddagger}$ (66.4 *vs.* 99.3 kJ mol^{-1}).

Predicting toxicity from hydrophobicity and reaction rate constant

As mentioned above, a major molecular mechanism resulting in a systematically enhanced toxicity of organic electrophiles is their covalent attack at nucleophilic protein sites.[13–17,32–34] In particular, it was shown recently that the combined use of experimentally determined log k_{GSH} and log K_{ow} (octanol/water partition coefficient, often used to convert external aqueous compound concentration to an estimated associated body burden) could explain the variation in Michael acceptor toxicity toward ciliates (*Tetrahymena pyriformis*, a unicellular aquatic organism), the latter of which was quantified through the compound concentration yielding 50% inhibition of their growth within 48 h exposure, EC_{50}.[15] Thus it was of interest to test the presently predicted $\Delta E^{\ddagger}$ and log k_{GSH} values for their suitability to add in the prediction of the aquatic toxicity of Michael acceptors.

With the two-variable regression model of Table 2 calibrated for 35 compounds, log k_{GSH} was predicted for all 47 α,β-unsaturated carbonyls of the present study (thus including 12 compounds without experimental log k_{GSH}) where experimental toxicity data in terms of 48-h log EC_{50} values for *Tetrahymena pyriformis* could be obtained from literature.[13,15,37–42] In this way, the GSH-calibrated Michael-acceptor reactivity of all compounds could be quantified through log k_{GSH} predicted from the two molecular properties $\Delta E^{\ddagger}$ and I_α as outlined above. Regression analyses of experimental log EC_{50} on (predicted)[43] log K_{ow} and (predicted) log k_{GSH} were performed separately for aldehydes, ketones and esters, following recent findings about the difference in impact of hydrophobicity and reactivity on toxicity between these three Michael-acceptor compound classes.[15]

The regression results are summarized in Table 4. For 16 aldehydes and 12 ketones, r^2 values > 0.9 and rms values around 0.2 log units are obtained, the latter of which are comparable to the estimated experimental log EC_{50} error (that is below 0.15 log units for the data from our lab, but not known for the other literature values). Note the significant difference in regression coefficients for log K_{ow} (–0.451 *vs.* –0.355) and log k_{GSH} (–0.509 *vs.* –0.568), reflecting the just mentioned difference in dependence of toxicity on hydrophobicity and electrophilic reactivity for these two classes of α,β-unsaturated carbonyls.

Concerning esters, exclusion of methyl tiglate improves r^2 from 0.75 to 0.82, and rms from 0.37 to 0.31 log units. Indeed it was shown earlier that for this compound, the Michael-acceptor reactivity is too low to affect its aquatic toxicity.[15] Note further that for the esters, the log K_{ow} regression coefficient is smaller and the log k_{GSH} regression coefficient larger than for both aldehydes and ketones, showing the larger reactivity impact on toxicity

Table 4 Regression models for predicting the ciliate toxicity of α,β-unsaturated aldehydes, esters and ketones from hydrophobicity and Michael-acceptor reactivity[a]

Compound class	n	a	b	c	r^2	rms	q^2_{cv}	rms_{cv}	$F_{2,n-3}$
$\log EC_{50}$ (mol L^{-1}) = $a \cdot \log K_{ow} + b \cdot \log k_{GSH}$ (L mol^{-1} min^{-1}) + c									
Aldehydes	16	−0.451 (± 0.058)	−0.509 (± 0.047)	−2.42 (± 0.14)	0.911	0.185	0.872	0.245	66.9
Ketones	12	−0.355 (± 0.106)	−0.568 (± 0.057)	−2.48 (± 0.22)	0.917	0.213	0.888	0.282	49.8
Ketones	11[b]	−0.359 (± 0.116)	−0.574 (± 0.072)	−2.46 (± 0.27)	0.890	0.222	0.814	0.332	32.2
Esters	19	−0.285 (± 0.131)	−0.578 (± 0.084)	−2.51 (± 0.22)	0.746	0.371	0.632	0.485	23.5
Esters	18[c]	−0.311 (± 0.114)	−0.678 (± 0.083)	−2.43 (± 0.19)	0.817	0.319	0.731	0.422	33.5

[a] The compounds and associated experimental log EC_{50} (mol L^{-1}) (48-h 50% growth inhibition of the ciliates *Tetrahymena pyriformis*) values[13,15,37–42] are listed in Table 1; log K_{ow} = calculated octanol/water partition coefficient;[45] log k_{GSH} is calculated from the two-variable model of Table 2 with 35 compounds (r^2 = 0.955, rms = 0.263), employing both the conformer-averaged (Boltzmann-weighted) protonated pathway Michael addition reaction barrier $\Delta E^{\ddagger}$ and the α-substitution indicator variable I_α. For n, a, b, c, r^2, rms, q^2_{cv}, rms_{cv}, and F, see legend of Table 2. [b] 3-Methyl-3-penten-2-one (as only α-substituted ketone; see Table 5 and text) excluded. [c] Methyl tiglate excluded (because its Michael-acceptor reactivity is too low to affect its aquatic toxicity).[17]

for this compound class. At present, the mechanistic reason for these (already previously) observed differences in impact of hydrophobicity and reactivity on the aquatic toxicity of α,β-unsaturated aldehydes, ketones and esters is not known.

In Fig. 2, the data distribution of predicted *vs.* experimental log EC_{50} is shown for all 46 compounds (excluding methyl tiglate, 7D), employing the three class-specific models of Table 4 for predicting log EC_{50} (50% growth inhibition of *Tetrahymena pyriformis* after 48-h exposure) from predicted log K_{ow} and predicted log k_{GSH}. The results thus demonstrate the feasibility of quantum chemically calculated electrophilicity in terms of rate constants of the reaction of Michael acceptors with a model nucleophile for predicting their toxicity in terms of 48-h 50% growth inhibition of the ciliates *Tetrahymena pyriformis*.

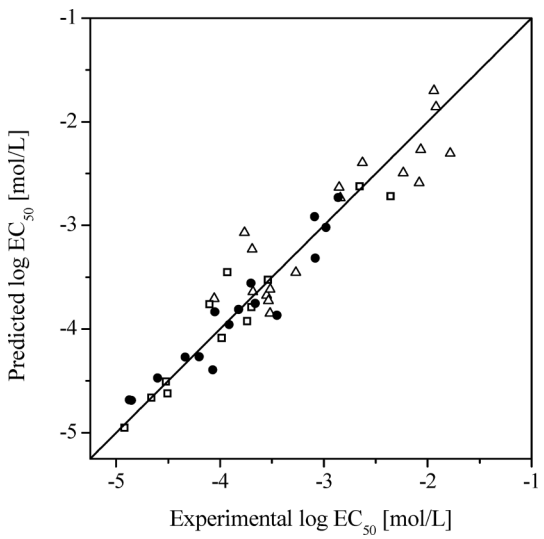

Fig. 2 Calculated *vs.* experimental log EC_{50} (mol L^{-1}) (48-h 50% growth inhibition of *Tetrahymena pyriformis*) for 46 α,β-unsaturated carbonyl compounds (excluding methyl tiglate, 7D, because of its too low reactivity; see text). Predicted values were calculated with the two-variable class-specific regression models from Table 4 for 16 aldehydes (filled circles; r^2 = 0.91, rms = 0.19, q^2_{cv} = 0.87, rms_{cv} = 0.25, $F_{2,13}$ = 67), 12 ketones (open squares; r^2 = 0.92, rms = 0.21, q^2_{cv} = 0.89, rms_{cv} = 0.28, $F_{2,9}$ = 50) and 18 esters (open triangles; r^2 = 0.82, rms = 0.32, q^2_{cv} = 0.73, rms_{cv} = 0.42, $F_{2,15}$ = 34).

Toxicity predicted from hydrophobicity and reaction barrier

Because log k_{GSH} is related to the reactive toxicity of Michael acceptors and can in turn be predicted from the reaction barrier $\Delta E^{\ddagger}$ and the α-substitution correction term I_α (see above and Table 2), the latter two molecular parameters may serve directly to predict, in combination with log K_{ow}, the ciliate toxicity in terms of log EC_{50}. The respective regression results are summarized in Table 5, again covering both class-specific and combined models.

For the 16 α,β-unsaturated aldehydes, the statistics are superior to the ones of Table 4, now yielding r^2 = 0.96 and rms = 0.13 log units. For all other subsets, the statistics are similar to the ones when employing predicted log k_{GSH} as regression variable (see Tables 4 and 5). Note further the similarity between the Table 4 and Table 5 models with regard to the log K_{ow} regression coefficient, showing in both cases a decrease in the impact of hydrophobicity on toxicity from aldehydes over esters to ketones. Correspondingly, the reactivity contribution to toxicity increases in this order across the compound classes as can be seen from the $\Delta E^{\ddagger}$ regression coefficients (0.0256 *vs.* 0.0319 *vs.* 0.0347; see Table 5). Because increasing $\Delta E^{\ddagger}$ lowers the reaction rate and thus the electrophilic reactivity of the Michael acceptor, its regression coefficient has a positive sign for predicting log EC_{50} (the larger log EC_{50}, the smaller the toxicity). By contrast, the log k_{GSH} regression coefficient is negative (Table 4), because here increasing log k_{GSH} raises reactivity and thus the reactive component of toxicity. In Fig. 3, the plot of predicted *vs.* experimental log EC_{50} employing calculated reaction barriers $\Delta E^{\ddagger}$ (instead of log k_{GSH}) is shown for all compounds except methyl tiglate (7D, because of its too low reactivity, s.a.).

Among the 12 ketones, 3-methyl-3-penten-2-one (4F) is the only compound with a substituent at the α-carbon, which makes the I_α regression coefficient of the ketone model less confident. Moreover, the number of 12 compounds would usually be considered to be too small for multilinear regression models employing three variables. Omission of this sole α-substituted derivative yields a two-variable regression model for 11 ketones with essentially identical regression coefficients for log K_{ow} and $\Delta E^{\ddagger}$ as well as for the intercept, which holds correspondingly with regard to log K_{ow}, log k_{GSH} and the intercept of the respective regression model of Table 4.

Table 5 Regression models for predicting the ciliate toxicity of α,β-unsaturated aldehydes, ketones and esters from hydrophobicity, intrinsic reaction barrier and the correction term for α-substitution[a]

Compound class	*n*	*a*	*b*	*c*	*d*	r^2	rms	q^2_{cv}	rms_{cv}	*F*
$\log EC_{50}$ (mol L^{-1}) = $a \cdot \log K_{ow} + b \cdot \Delta E^{\ddagger}$ (kJ mol^{-1}) + $c \cdot I_{\alpha} + d$										
Aldehydes	16	−0.412 (± 0.044)	0.0256 (± 0.0021)	0.87 (± 0.08)	−5.00 (± 0.13)	0.956	0.130	0.920	0.193	85.7
Ketones	12	−0.359 (± 0.116)	0.0319 (± 0.0040)	0.67 (± 0.29)	−5.37 (± 0.26)	0.917	0.212	—	—	29.6
Ketones	11[b]	−0.359 (± 0.116)	0.0319 (± 0.0040)	—	−5.37 (± 0.26)	0.890	0.222	0.814	0.332	32.2
Esters	19	−0.258 (± 0.148)	0.0303 (± 0.0064)	0.81 (± 0.23)	−5.35 (± 0.50)	0.749	0.369	0.599	0.506	15.0
Esters	18[c]	−0.266 (± 0.126)	0.0347 (± 0.0057)	1.00 (± 0.21)	−5.73 (± 0.45)	0.826	0.311	0.720	0.430	22.2

[a] The compounds and associated experimental log EC_{50} (mol L^{-1}) (48-h 50% growth inhibition of the ciliates *Tetrahymena pyriformis*) values[13,15,37–42] are listed in Table 1; log K_{ow} = calculated octanol/water partition coefficient.[45] $\Delta E^{\ddagger}$ (kJ mol^{-1}) = B3LYP/6-31G** conformer-averaged (Boltzmann-weighted) protonated pathway reaction barrier of the Michael addition of CH_3SH; I_{α} = indicator variable discriminating between the absence ($I_{\alpha} = 0$) and presence ($I_{\alpha} = 1$) of a substituent at the α-carbon of the Michael acceptor; *a*, *b*, *c*, *d* = regression parameters; *n* = number of compounds, r^2 = squared correlation coefficient, rms = root-mean-square error, q^2_{cv} = leave-one-out cross-validated correlation coefficient,[50] rms_{cv} = leave-one-out cross-validated root-mean-square error, *F* = *F*-test value referring to three ($F_{3,n-4}$) or four ($F_{4,n-5}$) regression variables. [b] 3-Methyl-3-penten-2-one (as only α-substituted ketone; see text) excluded. [c] Methyl tiglate excluded (because its Michael-acceptor reactivity is too low to affect its aquatic toxicity).[17]

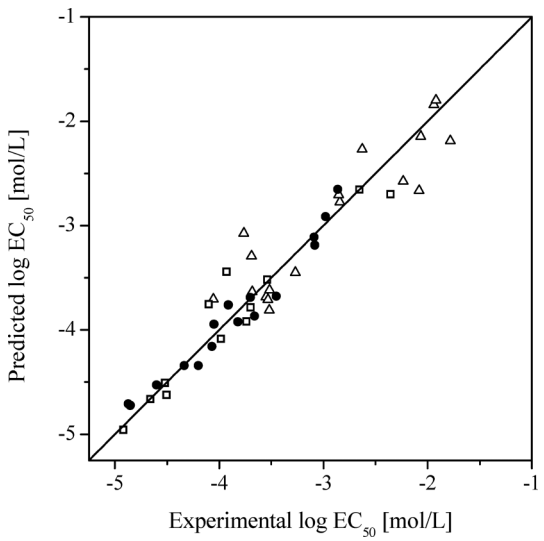

Fig. 3 Calculated *vs.* experimental log EC_{50} (mol L^{-1}) (48-h 50% growth inhibition of *Tetrahymena pyriformis*) for 46 α,β-unsaturated carbonyl compounds (excluding methyl tiglate, 7D, because of its too low reactivity; see text). Predicted values were calculated with the three-variable class-specific regression models from Table 5 for 16 aldehydes (filled circles; r^2 = 0.96, rms = 0.13, q^2_{cv} = 0.92, rms_{cv} = 0.19, $F_{3,12}$ = 86), 12 ketones (open squares; r^2 = 0.92, rms = 0.21, $F_{3,8}$ = 30) and 18 esters (open triangles; r^2 = 0.83, rms = 0.31, q^2_{cv} = 0.72, rms_{cv} = 0.43, $F_{3,14}$ = 22).

Overall, the present findings show that for α,β-unsaturated aldehydes, ketones and esters, the *in vitro* toxicity in terms of log EC_{50} can be well predicted from quantum chemically calculated reaction barriers when combined with log K_{ow} and an indicator variable discriminating between α-substituted and α-H derivatives. In particular, the high level of correlation for both Michael-acceptor reactivity and toxicity obtained with intrinsic (Boltzmann-weighted) reaction barriers $\Delta E^{\ddagger}$ is remarkable, considering the fact that solvation effects have not been taken into account. Note further that in contrast to the α-substitution effect, the significant lowering of Michael-acceptor reactivity through β-substitution is well captured by $\Delta E^{\ddagger}$. The unresolved α-substitution effect suggests a catalytic support of the Michael addition through water, which may be subject to future investigations.

Conclusions

For the predictive assessment and mechanistic analysis of the toxicity of α,β-unsaturated carbonyls, information about their electrophilic reactivity is crucial. The presently derived quantum chemical approach for predicting the Michael-acceptor reactivity from transition-state energies appears useful as in silico tool of integrated testing strategies for human and environmental toxicology endpoints in the context of the European REACH and Cosmetics Directives, and provides excellent statistics with a single model across aldehydes, ketones and esters (r^2 = 0.96). The predictive power of this approach is further illustrated by its successful application for predicting the aquatic toxicity of an augmented set of α,β-unsaturated carbonyls when combined with hydrophobicity, providing the first model of its kind (with r^2 values up to 0.96, 0.92 and 0.83 for aldehydes, ketones and esters, respectively). Concerning the reaction mechanism of the Michael addition, our computational analysis suggests that the direct 1,2-addition across the electron-poor double bond $C_{\alpha}{=}C_{\beta}$ of Michael acceptors may be a viable alternative to the often discussed conjugated 1,4-addition pathway, keeping in mind that a more comprehensive mechanistic analysis would require an appropriate account of solvation.

Computational methods

Compounds and experimental data

The compound set consists of 47 α,β-unsaturated carbonyls, covering 16 aldehydes, 12 ketones and 19 esters. Associated toxicity information in terms of compound concentrations yielding 50% growth inhibition of the ciliates *Tetrahymena pyriformis* after 48 h exposure (log EC_{50} (mol L^{-1})) was taken from literature.[13,15,37–42] For a subset of 35 compounds (10 aldehydes, 11 ketones, 14 esters), experimental 2nd-order rate constants of their reaction with glutathione (GSH) in logarithmic form, log k_{GSH} (L mol^{-1} min^{-1}), were available from our previous work employing the kinetic GSH chemoassay.[14,15,32] For the remaining 12 Michael acceptors, log

k_{GSH} was predicted with a regression model calibrated for the 35-compound subset as outlined below and summarized in the last row of Table 2. Log K_{ow} values were calculated for all 47 compounds using KOWWIN v 1.67.[43]

Quantum chemical calculations

For the computational analysis of the differences in electrophilic reactivity of the Michael acceptors in terms of their log k_{GSH} values, the model nucleophile methane thiol (CH_3SH) was employed as surrogate for GSH. Gaussian 03[44] was used for all quantum chemical calculations including geometry optimization at the density functional theory (DFT) level, employing the B3LYP[45,46] hybrid functional and the 6-31G** basis set.[47] Harmonic vibrational frequencies were calculated for all stationary points using analytical gradients, confirming both true minima (no imaginary frequency) for the ground-state geometries of methane thiol as well as for all 47 α,β-unsaturated carbonyls and their protonated derivatives (adding H^+ to the carbonyl oxygen) in all relevant conformations considered (see below), and 1st-order saddle points (one imaginary frequency) for the transition states of the respective electrophile-nucleophile reactions. The latter refer to the 1,2-olefin addition mechanism with initial attack of the thiol sulphur at the β-carbon of the Michael acceptor, considering both the neutral and protonated Michael acceptor as reactant (see Scheme 2). For all ground-state geometries, the Gibbs free energy G was calculated including the zero-point vibrational energy and thermal corrections based on ideal gas behaviour with a temperature of $T = 298.15$ K. No frequency scaling was applied in calculating G. The effect of bulk solvation was explored through single-point calculations using the polarisable continuum model (PCM) as implemented in Gaussian, applying $\varepsilon = 78.39$ for aqueous solvation and the standard setting for the cavity construction with UAHF atomic radii.

Relationship between reaction barrier and rate constant

The free energy of activation, $\Delta G^{\ddagger}$, is related to the rate constant of a biomolecular elementary reaction through the Eyring equation

$$k = \frac{k_B T}{h} \cdot \frac{1}{c^0} \exp\left(-\frac{\Delta G^{\ddagger}}{RT}\right) \quad (3)$$

where k is the rate constant of interest, k_B the Boltzmann constant, h the Planck constant, R the gas constant, T the temperature, and c^0 the concentration defining the standard state (typically 1 mol L^{-1}). In our case, $\Delta G^{\ddagger}$ was approximated by the reaction barrier $\Delta E^{\ddagger}$, because the harmonic oscillator approximation used for calculating frequencies becomes increasingly less suited for increasingly soft vibrational modes, resulting in increasingly large errors in the thermal correction. $\Delta E^{\ddagger}$ was used for predicting log k_{GSH} through a linear regression (see below), thus compensating for the various approximations involved (gas-phase quantum chemistry, reactant CH_3SH instead of GSH, and $\Delta E^{\ddagger}$ instead of $\Delta G^{\ddagger}$), and omitting the need for specifying the standard state. The conformational flexibility of the reactants was accounted for through employing Boltzmann-weighted $\Delta E^{\ddagger}$ values (see eqn (1) and (2) above).

Regression analyses

Linear regression equations were derived for predicting log k_{GSH} (L mol^{-1} min^{-1}) from calculated $\Delta E^{\ddagger}$ (kJ mol^{-1}), and for predicting log EC_{50} (mol L^{-1}) through a combination of predicted log k_{GSH} or $\Delta E^{\ddagger}$ and log K_{ow}. To this end, an indicator variable I_{α} was included to differentiate between α-substituted ($I_{\alpha} = 1$) and α-H ($I_{\alpha} = 0$) Michael-acceptor carbonyls (see also main text above).

The statistical performance was characterized in terms of the following parameters: Squared correlation coefficient, r^2; leave-one-out cross-validated squared correlation coefficient, q^2_{cv};[48] root-mean-square error of calibration, rms; leave-one-out cross-validated root-mean-square error, rms_{cv}; F-test value, $F_{i,n-(i+1)}$ (with i = number of variables, and n = number of compounds).

Funding Support

Financial support from the EU project OSIRIS (No. GOCE-CT-2007-037017) is gratefully acknowledged.

References

1 Y. Takemoto, Recognition and activation by ureas and thioureas: stereoselective reactions using ureas and thioureas as hydrogen-bonding donors, *Org. Biomol. Chem.*, 2005, **3**, 4299–4306.
2 J. Liu, Z. Yang, X. Liu, Z. Wang, Y. Liu, A. Bai, L. Lin and X. Feng, Organocatalyzed highly stereoselective Michael addition of ketones to alkylidene malonates and nitroolefins using chiral primary-secondary diamine catalysts based on bispidine, *Org. Biomol. Chem.*, 2009, **7**, 4120–4127.
3 T.-R. Kang, J.-W. Xie, W. Du, X. Feng and Y.-C. Chen, Stereoselective desymmetrisation of prochiral α,α-dicyanoalkenes *via* domino Michael–Michael addition reactions, *Org. Biomol. Chem.*, 2008, **6**, 2673–2675.
4 F. Bonfils, I. Cazaux, P. Hodge and C. Caze, Michael reactions carried out using a bench-top flow system, *Org. Biomol. Chem.*, 2006, **4**, 493–497.
5 E. Lewandowska, Substitution at the α-carbons of α,β-unsaturated carbonyl compounds: anti-Michael addition, *Tetrahedron*, 2007, **63**, 2107–2122.
6 B. D. Mather, K. Viswanathan, K. M. Miller and T. E. Long, Michael addition reactions in macromolecular design for emerging technologies, *Prog. Polym. Sci.*, 2006, **31**, 487–531.
7 E. C. Miller and J. A. Miller, Searches For Ultimate Chemical Carcinogens And Their Reactions With Cellular Macromolecules, *Cancer*, 1981, **47**, 2327–2345.
8 B. Coles and B. Ketterer, The Role of Glutathione and Glutathione Transferases in Chemical Carcinogenesis, *Crit. Rev. Biochem. Mol. Biol.*, 1990, **25**, 47–70.
9 A. Benigni and C. Bossa, Mechanisms of Chemical Carcinogenicity and Mutagenicity: A Review with Implications for Predictive Toxicology, *Chem. Rev.*, 2011, **111**, 2507–2536.
10 A. K. Smith and S. A. M. Hotchkiss, *Allergic Contact Dermatitis*, Taylor & Francis, London, UK, 2001.
11 A. T. Karlberg, M. A. Bergström, A. Börje, K. Luthman and J. L. G. Nilsson, Allergic contact dermatitis – formation, structural requirements, and reactivity of skin sensitizers, *Chem. Res. Toxicol.*, 2008, **21**, 53–69.
12 H. Alenuis, D. W. Roberts, Y. Tokura, A. Lauerma, G. Patlewicz and M. S. Roberts, Skin, drug and chemical reactions, *Drug Discovery Today Dis. Mech.*, 2008, **5**, e211–e220.
13 A. O. Aptula and D. W. Roberts, Mechanistic Applicability Domains for Nonanimal-Based Prediction of Toxicological End Points: General Principles And Application to Reactive Toxicity, *Chem. Res. Toxicol.*, 2006, **19**, 1097–1105.
14 A. Böhme, D. Thaens, A. Paschke and G. Schüürmann, Kinetic Glutathion Chemoassay To Quantify Thiol Reactivity of Organic Electrophiles – Application to α,β-Unsaturated Ketones, Acrylates, and Propiolates, *Chem. Res. Toxicol.*, 2009, **22**, 742–750.

15 A. Böhme, D. Thaens, F. Schramm, A. Paschke and G. Schüürmann, Thiol Reactivity and its Impact on the Ciliate Toxicity of α,β-Unsaturated Aldehydes, Ketones and Esters, *Chem. Res. Toxicol.*, 2010, **23**, 1905–1912.
16 U. Blaschke, A. Paschke, I. Rensch and G. Schüürmann, Acute and Chronic Toxicity toward the Bacteria *Vibrio fischeri* of Organic Narcotics and Epoxides: Structural Alerts for Epoxide Excess Toxicity, *Chem. Res. Toxicol.*, 2010, **23**, 1936–1946.
17 F. Schramm, A. Müller, H. Hammer, A. Paschke and G. Schüürmann, Epoxide and Thiirane Toxicity In vitro with the Ciliates *Tetrahymena pyriformis*: Structural Alerts Indicating Excess Toxicity, *Environ. Sci. Technol.*, 2011, **45**, 5812–5189.
18 K. Uchida, S. Toyokuni, K. Nishikawa, S. Kawakishi, H. Oda, H. Hiai and E. R. Stadtman, Michael Addition-Type 4-Hydroxy-2-nonenal Adducts in Modified Low-Density Lipoproteins: Markers for Atherosclerosis, *Biochemistry*, 1994, **33**, 12487–12494.
19 D. A. Butterfield, A. Castegna, C. M. Lauderback and J. Drake, Evidence that amyloid beta-peptide-induced lipid peroxidation and its sequelae in Alzheimer's disease brain contribute to neuronal death, *Neurobiol. Aging*, 2002, **23**, 655–664.
20 A.-L. Levonen, A. Landar, A. Ramachandran, E. K. Ceaser, D. A. Dickinson, G. Zanoni, J. D. Morrow and V. M. Darley-Usmar, Cellular mechanisms of redox cell signalling: role of cysteine modification in controlling antioxidant defences in response to electrophilic lipid oxidation products, *Biochem. J.*, 2004, **378**, 373–382.
21 D. Méndez, M. L. Hernáez, A. Diez, A. Puyet and J. M. Bautista, Combined Proteomic Approaches for the Identification of Specific Amino Acid Residues Modified by 4-Hydroxy-2-Nonenal under Physiological Conditions, *J. Proteome Res.*, 2010, **9**, 5770–5781.
22 M. E. Szapacs, J. N. Riggins, L. J. Zimmerman and D. C. Liebler, Covalent Adduction of Human Serum Albumin by 4-Hydroxy-2-Nonenal: Kinetic Analysis of Competing Alkylation Reactions, *Biochemistry*, 2006, **45**, 10521–10528.
23 A. Rossi, P. Kapahi, G. Natoli, T. Takahashi, Y. Chen, M. Karin and M. G. Santoro, Anti-inflammatory cyclopentenone prostaglandins are direct inhibitors of IκB kinase, *Nature*, 2000, **403**, 103–108.
24 L. J. Macpherson, A. E. Dubin, M. J. Evans, F. Marr, P. G. Schultz, B. F. Cravatt and A. Patapoutian, Noxious compounds activate TRPA1 ion channels through covalent modification of cysteines, *Nature*, 2007, **445**, 541–545.
25 A. T. Dinkova-Kostova, M. A. Massiah, R. E. Bozak, R. J. Hicks and P. Talalay, Potency of Michael reaction accepters as inducers of enzymes that protect against carcinogenesis depends on their reactivity with sulfhydryl groups, *Proc. Natl. Acad. Sci. U. S. A.*, 2001, **98**, 3404–3409.
26 O. Mekenyan, G. Patlewicz, G. Dimitrova, C. Kuseva, M. Todorov, S. Stoeva, S. Kotov and E. M. Donner, Use of Genotoxicity Information in the Development of Integrated Testing Strategies (ITS) for Skin Sensitization, *Chem. Res. Toxicol.*, 2010, **23**, 1519–1540.
27 A. Paasche, M. Schiller, T. Schirmeister and B. Engels, Mechanistic Study of the Reaction of Thiol-Containing Enzymes with α,β-Unsaturated Carbonyl Substrates by Computation and Chemoassays, *ChemMedChem*, 2010, **5**, 869–880.
28 L. H. Um, E. J. Lee and J. S. Min, Remarkable catalytic effect of H^+ in Michael-type additions of anilines to 3-butyn-2-one, *Tetrahedron*, 2001, **57**, 9585–9589.
29 M. Aleksic, E. Thain, D. Roger, O. Saib, M. Davies, J. Li, A. Aptula and R. Zazzeroni, Reactivity Profiling: Covalent Modification of Single Nucleophile Peptides for Skin Sensitization Risk Assessment, *Toxicol. Sci.*, 2009, **108**, 401–411.
30 D. W. Roberts and A. Natsch, High Throughput Kinetic Profiling Approach for Covalent Binding to Peptides: Application to Skin Sensitization Potency of Michael Acceptor Electrophiles, *Chem. Res. Toxicol.*, 2009, **22**, 592–603.
31 J. F. Lalko, I. Kimber, R. J. Dearman, G. F. Gerberick, K. Sarlo and A. M. Api, Chemical reactivity measurements: Potential for characterization of respiratory chemical allergens, *Toxicol. in Vitro*, 2011, **25**, 433–445.
32 D. Wondrousch, A. Böhme, D. Thaens, N. Ost and G. Schüürmann, Local Electrophilicity Predicts the Toxicity-Relevant Reactivity of Michael Acceptors, *J. Phys. Chem. Lett.*, 2010, **1**, 1605–1610.
33 J. A. H. Schwöbel, D. Wondrousch, Y. K. Koleva, J. C. Madden, M. T. D. Cronin and G. Schüürmann, Prediction of Michael-Type Acceptor Reactivity toward Glutathione, *Chem. Res. Toxicol.*, 2010, **23**, 1576–1585.
34 J. A. H. Schwöbel, J. C. Madden and M. T. D. Cronin, Examination of Michael addition reactivity towards glutathione by transition-state calculations, *SAR QSAR Environ. Res.*, 2010, **21**, 693–710.
35 Z. Kunakbaeva, R. Carrasco and I. Rozas, An approximation to the mechanism of inhibition of cystein proteases: nucleophilic sulphur addition to Michael acceptors type compounds, *THEOCHEM*, 2003, **626**, 209–216.
36 L. Pardo, R. Osman, H. Weinstein and J. R. Rabinowitz, Mechanisms Of Nucleophilic-Addition To Activated Double-Bonds – 1,2-Michael And 1,4-Michael Addition Of Ammonia, *J. Am. Chem. Soc.*, 1993, **115**, 8263–8269.
37 T. W. Schultz, T. I. Netzeva, D. W. Roberts and M. T. D. Cronin, Structure-Toxicity Relationship for the Effects to *Tetrahymena pyriformis* of Aliphatic, Carbonyl-Containing, α,β-Unsaturated Chemicals, *Chem. Res. Toxicol.*, 2005, **18**, 330–341.
38 J. W. Yarbrough and T. W. Schultz, Abiotic Sulfhydryl Reaktivity: A Predictor of Aquatic Toxicity for Carbonyl-Containing α,β-Unsaturated Compounds, *Chem. Res. Toxicol.*, 2007, **20**, 558–562.
39 Y. K. Koleva, J. C. Madden and M. T. D. Cronin, Formation of Categories from Structure–activity Relationship To Allow Read-Across for Risk Assessment: Toxicity of α,β-Unsaturated Carbonyl Compounds, *Chem. Res. Toxicol.*, 2008, **21**, 2300–2312.
40 T. W. Schultz and J. W. Yarbrough, Trends in structure-toxicity relationship for carbonyl-containing α,β-unsaturated compounds, *SAR QSAR Environ. Res.*, 2004, **15**, 139–146.
41 A. P. Bearden and T. W. Schultz, Comparison of *Tetrahymena* and *Pimephales* toxicity based on mechanism of action, *SAR QSAR Environ. Res.*, 1998, **9**, 127–153.
42 T. I. Netzeva, T. W. Schultz, A. O. Aptula and M. T. D. Cronin, Partial least squares modelling of the acute toxicity of aliphatic compounds to *Tetrahymena pyriformis*, *SAR QSAR Environ. Res.*, 2003, **14**, 265–283.
43 W. M. Meylan, *KOWWIN 1.67*, Syracuse Research Corporation, Syracuse NY, USA, 2004.
44 M. J. Frisch, G. W. Trucks, H. B. Schlegel, G. E. Scuseria, M. A. Robb, J. R. Cheeseman, J. A. Montgomery, Jr., T. Vreven, K. N. Kudin, J. C. Burant, J. M. Millam, S. S. Iyengar, J. Tomasi, V. Barone, B. Mennucci, M. Cossi, G. Scalmani, N. Rega, G. A. Petersson, H. Nakatsuji, M. Hada, M. Ehara, K. Toyota, R. Fukuda, J. Hasegawa, M. Ishida, T. Nakajima, Y. Honda, O. Kitao, H. Nakai, M. Klene, X. Li, J. E. Knox, H. P. Hratchian, J. B. Cross, V. Bakken, C. Adamo, J. Jaramillo, R. Gomperts, R. E. Stratmann, O. Yazyev, A. J. Austin, R. Cammi, C. Pomelli, J. Ochterski, P. Y. Ayala, K. Morokuma, G. A. Voth, P. Salvador, J. J. Dannenberg, V. G. Zakrzewski, S. Dapprich, A. D. Daniels, M. C. Strain, O. Farkas, D. K. Malick, A. D. Rabuck, K. Raghavachari, J. B. Foresman, J. V. Ortiz, Q. Cui, A. G. Baboul, S. Clifford, J. Cioslowski, B. B. Stefanov, G. Liu, A. Liashenko, P. Piskorz, I. Komaromi, R. L. Martin, D. J. Fox, T. Keith, M. A. Al-Laham, C. Y. Peng, A. Nanayakkara, M. Challacombe, P. M. W. Gill, B. G. Johnson, W. Chen, M. W. Wong, C. Gonzalez and J. A. Pople, *GAUSSIAN 03 (Revision C.02)*, Gaussian, Inc., Wallingford, CT, 2004.
45 C. T. Lee, W. T. Yang and R. G. Parr, Development Of The Colle-Salvetti Correlation-Energy Formula Into A Functional Of The Electron-Density, *Phys. Rev. B*, 1988, **37**, 785–789.
46 A. D. Becke, A New Mixing Of Hartree–Fock And Local Density-Functional Theories, *J. Chem. Phys.*, 1993, **98**, 1372–1377.
47 W. J. Hehre, L. Radom, P. v. R. Schleyer and J. A. Pople, *Ab Initio Molecular Orbital Theory*, Wiley, New York, USA, 1986.
48 G. Schüürmann, R. U. Ebert, W. J. Chen, B. Wang and R. Kühne, External Validation and Prediction Employing the Predictive Squared Correlation Coefficient - Test Set Activity Mean *vs.* Training Set Activity Mean, *J. Chem. Inf. Model.*, 2008, **48**, 2140–2145.

